A Density-Functional Theory Investigation of the Radiation Products of L-α-Alanine

Fuqiang Ban, Stacey D. Wetmore, and Russell J. Boyd*

Department of Chemistry, Dalhousie University, Halifax, NS, Canada B3H 4J3

Received: January 22, 1999

Density-functional theory is used to investigate the radiation products (radicals R1, $^{\bullet}CH(CH_3)COOH$; R2, $H_3N^+C^{\bullet}(CH_3)COO^-$; and R3, $H_2NC^{\bullet}(CH_3)COOH$) of L-α-alanine at 295 K. Four conformers were found for R1 and R3. A planar structure of R2 in a zwitterionic form was obtained with the Onsager model. The relative energies of each of the four conformers of R1 and R3 show that structures with intramolecular hydrogen bonding are more stable. The computed hyperfine couplings are shown to be in good agreement with the accurate results obtained from the electron paramagnetic resonance (EPR), electron−nuclear double resonance (ENDOR), and EIE (ENDOR-induced EPR) experiments performed by Sagstuen et al. [Sagstuen, E.; Hole, E. O.; Haugedal, S. R.; Nelson, W. H. *J. Phys. Chem. A* **1997**, *101*, 9763]. The effects of rotation about the NC_2 bond on the HFCCs of the amino protons in R2 support the previous suggestion that the amino protons are fixed by intermolecular hydrogen bonding in L-α-alanine crystals. Moreover, a good correlation between the structure of the amino group and HFCCs in the four conformers of R3 was found.

Introduction

Amino acids were among the first irradiated biomolecules to be studied by the technique of electron spin resonance spectroscopy. Fundamental work on X- and γ-irradiated single crystals of amino acids remains an active field.[1,2] Many studies of the radicals generated by irradiation of L-α-alanine have been published.[3−15] Particular interest in L-α-alanine has arisen due to its radiation dosimetric properties. Initial studies assumed that the solid radical population in L-α-alanine consisted of only one radical (R1), and all variations in the spectra were assigned to various properties of this radical.[16−18] Also in several spin-trapping studies[19,20] of alanine radicals formed in polycrystalline samples, only R1 was detected. However, it has been suggested[3,13,16−18,21,22] that the spectra of several radicals could be overlapping. This hypothesis was proven by Sagstuen et al.[2] In their study, two new radicals were clearly detected by a combination of EPR (electron paramagnetic resonance), ENDOR (electron−nuclear double resonance), and EIE (ENDOR-induced EPR) techniques. Thus, to date three radicals have been found upon the X irradiation of L-α-alanine crystals at 295 K. The radical structures were tentatively assigned to be those displayed in Figure 1.

From a simulated spectrum,[2] it was concluded that radicals R1 and R2 are present in comparable amounts (with an approximate ratio of 60% to 40%). R3 was recognized as a minor species. It was estimated that the α-C spin density of the two proposed conformers should be on the order of 35−40%. R1 is a deamination product, R2 is a hydrogen-abstraction product, and R3 is a hydrogen-abstraction accompanied by a proton-transfer product. Alternatively, R3 could be generated from R2 as will be proposed in a later section. In the radiation chemistry of amino acids, the deamination product can be formed from a protonated anion through a reductive pathway, while the oxidation product can be formed from a cation. In L-α-alanine crystals irradiated at 77 K, an unusual cation[10] has been postulated to explain the ESR spectrum of the oxidation product, but the oxidation product has not been detected. It seems that all radicals generated in irradiated L-α-alanine crystals at 295 K follow the reductive path. However, since the oxidation radical is very unstable,[23,24] it can abstract hydrogen from an alanine molecule to form R2, and the oxidative radiation-induced pathway cannot be excluded. Thus, the mechanism leading to R2 is still controversial.[2]

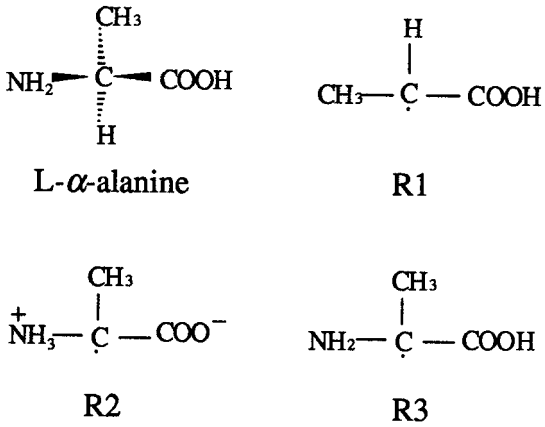

Figure 1. Structure of L-α-alanine and the proposed radicals formed upon X irradiation of L-α-alanine crystals at 295 K.

Amino acids are the building blocks of proteins, and they exist as zwitterionic species in the crystalline state and in solution. When irradiated, radicals in a zwitterionic form (such as R2 in L-α-alanine) can be formed. The zwitterionic structure of amino acids and their derived radicals has been a challenge for theoretical chemistry. In the past few years, many theoretical papers have been devoted to the investigation of amino acids in their zwitterionic structures.[25−29] For the simplest amino acid glycine, ab initio calculations[30] using large basis sets show that the zwitterionic form is not a minimum in vacuo. Similarly, the zwitterionic form does not correspond to a stationary point for an isolated glycine radical.[31,32] Thus, to explore the zwitterionic form of amino acids, environmental effects must be taken into account.

There are two strategies to account for environmental effects. One is to build a model by adding discrete molecules around the target molecule. The second strategy is to use a continuum

10.1021/jp990257n CCC: $18.00
Published on Web 05/08/1999

model where a target molecule is placed in a cavity surrounded by a continuum (such as the standard Onsager model,[33,34] in which the molecule is surrounded by a uniform dielectric that produces an electric field on the molecule). Detailed studies[27,28] on the zwitterionic forms of glycine and alanine in solution show that the continuum model provides reliable zwitterionic structures for amino acids. Three papers[31,32,35] focused on calculating the structure and ESR features of a glycine radical in its zwitterionic form. In particular, one DFT study[35] showed that the magnetic properties of the glycine radical in its zwitterionic form are scarcely affected by the crystalline environment. The ESR spectra for the system investigated were well reproduced by dynamic computations on the isolated radical structure obtained in a polar environment described by the conductive-like polarizable continuum model.

Amino acid radicals are involved in many biological reactions.[36−38] Considerable attention has been focused on the formation, stability, and reactions of protein radicals in biological systems.[38] The oxidative damage to amino acids is of importance in pharmacology and pathology.[39] Great effort[13] has been made to obtain a rough estimate of the coordinates of R1 in a unit cell. In addition, a few considerations[2] of the geometrical conformation of R2 have been made by considering the Heller−McConnell relation.[40] However, relatively less information is available for the structures of R2 and R3. Since the assignment of complicated ESR spectra often requires simulations obtained under some assumptions, the theoretical prediction of coupling constants in amino acid radiation products may be able to provide valuable support for experimental results.

Density-functional theory (DFT) has been shown to yield very accurate hyperfine coupling constants (HFCCs) at a fraction of the computational cost of the other methods appropriate for the calculation of this property.[41,42] In addition, extensive DFT studies[43] on the radicals formed in irradiated DNA bases and the sugar moiety show the strength of DFT methods for the study of biological systems. This prompts the present systematic study on amino acid radicals using DFT in order to gain a better understanding of the reactions in X-irradiated crystals of L-α-alanine.

Computational Details

In the present study, all geometry optimizations were performed with the B3LYP hybrid functional in conjunction with Pople's 6-31+G(d,p) basis set. The B3LYP functional is a combination of Becke's three-parameter hybrid exchange functional[44] and the Lee−Yang−Parr correlation functional.[45] Since it was previously shown[26] that the geometry of the zwitterionic structure for glycine obtained with the Onsager model is very close to that found using a model based on the multipolar moment, the zwitterionic structure of radical R2 was optimized using the standard Onsager model with a dielectric constant (ϵ) of 78.39 and an estimated radius of 3.76 Å for the fixed spherical cavity. All geometry optimizations were accomplished using Gaussian 94.[46] Single-point calculations at the B3LYP level with Pople's 6-311G(2df,p) basis set were performed on each of the four conformers of R1 and R3 to obtained their relative energies. The zero-point energy correction was included in all relative energies. All stationary points on the potential energy surfaces were confirmed to be local minima by frequency calculations. The hyperfine coupling constants were obtained with the PWP86 functional which is a combination of Perdew and Wang's exchange functional (PW)[47] and Perdew's nonlocal correlation functional (P86).[48] The PWP86 calculations were carried out using the deMon[49] program with the 6-311G(2d,p) basis set to obtain isotropic and anisotropic hyperfine coupling constants. The (5,4;5,4) family of auxiliary basis sets was used to fit the charge density and the exchange correlation potential. This functional and basis set combination has been found to yield hyperfine coupling constants of very high accuracy in studies of histidine[50] and model π-radicals.[51] It should be noted that a mixture of computational techniques is used in the present study since accurate geometries can be obtained with smaller basis sets while HFCCs require larger, more complete basis sets. The implementation of a small basis set for geometry optimizations greatly reduces the computational time.

The molecular EPR hyperfine splittings are caused by the magnetic interaction between the nuclear spin and the electronic magnetic moments. The splitting can be separated into an isotropic part and an anisotropic part. For a particular nucleus N, the isotropic coupling depends on the unpaired spin density, $\rho^{\alpha-\beta}(0)$, at the position of the nucleus only and can be calculated through the following equation

$$A_{\mathrm{iso}} = \frac{8\pi}{3} g\beta g_{\mathrm{N}}\beta_{\mathrm{N}}\rho^{\alpha-\beta}(0)$$

where g and β are the electronic g-factor and the Bohr magneton, respectively, and g_{N} and β_{N} are the corresponding nuclear factors. The anisotropic coupling is related to the interactions between magnetic dipoles, and the ijth component of the anisotropic tensor can be evaluated by the classical expression for interacting dipoles

$$T_{ij} = \frac{1}{2} g\beta g_{\mathrm{N}}\beta_{\mathrm{N}}\langle S_Z\rangle^{-1}\sum_{\mu\nu}\rho_{\mu\nu}^{\alpha-\beta}\langle\phi_\mu|r_{\mathrm{kN}}{}^{-5}(r_{\mathrm{kN}}{}^{2}\delta_{ij} - 3r_{\mathrm{kN},i}r_{\mathrm{kN},j})|\phi_\nu\rangle$$

where $\rho_{\mu\nu}^{\alpha-\beta}$ is an element of the spin density matrix. The full coupling tensor of the nucleus of interest in the principal axes is calculated by the addition of the isotropic HFCC to each component of the anisotropic tensor ($A_{ii} = A_{\mathrm{iso}} + T_{ii}$).

Results and Discussion

Geometry. The molecular structures of R1, R2, and R3 were fully optimized at the B3LYP/6-31+G(d,p) level. Four different minima for both R1 (Figure 2) and R3 (Figure 4) were found due to the fact that the proton has two possible positions on each of the oxygen atoms in the carboxylate group. Only one minimum of the zwitterionic form of R2 (Figure 3) was found using the standard Onsager model. Select geometrical parameters of R1, R2, and R3 are shown in Figures 2, 3, and 4, respectively. The relative energies of the four conformers of R1 and R3 are shown in Table 1. Complete geometries and energies can be obtained as Supporting Information. All four structures of R1 and the zwitterionic structure of R2 have a planar skeleton (except for the hydrogen atoms in the methyl and amino groups). Thus, R1 and R2 are typical π-radicals. On the other hand, in all four structures of R3, the nitrogen atom sticks out of the $C_1C_2C_3$ plane by 3.2°−6.4°. Thus, the structures of R3 are slightly pyramidal. The main differences in the four structures of R1 caused by the arrangement of the OH_x bond are the reorganization of the atoms in the molecular plane. The largest changes are 0.028 Å in bond length (CO bond) and 11.6° in bond angle ($\angle O_1C_1C_2$). From the relative energies, it can be seen that R1-II and R1-IV with intramolecular hydrogen bonding are more stable than R1-I and R1-III. Also, it can be seen that in R1-III the interaction between H_x and the methyl group causes

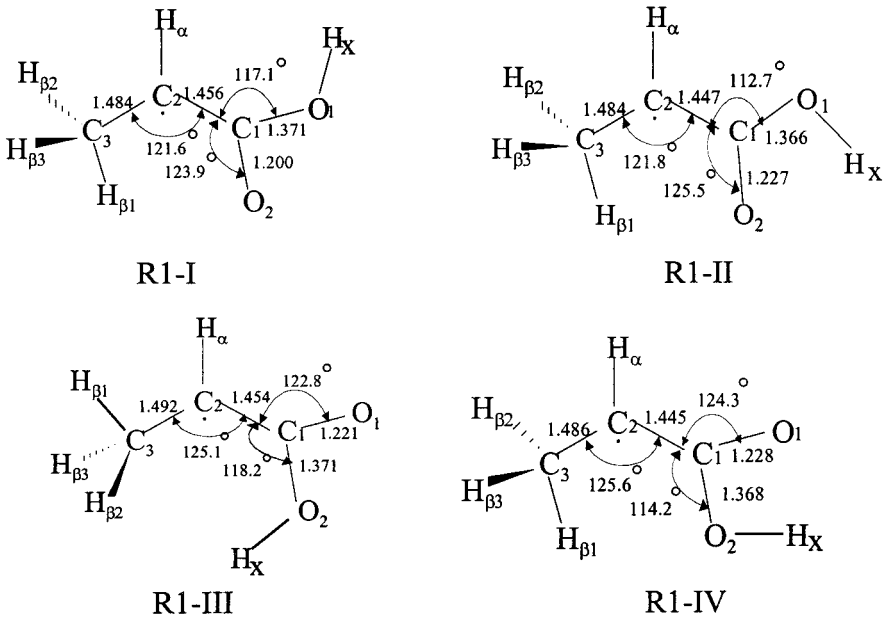

Figure 2. Optimized structures for R1 at the B3LYP/6-31+G(d,p) level (bond angles are recorded in degrees and bond lengths in angstroms).

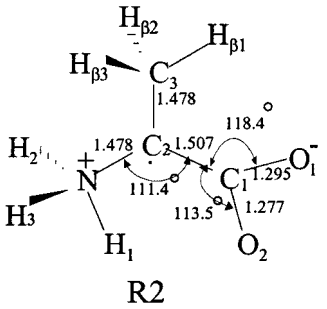

Figure 3. Optimized structure of R2 at the B3LYP/6-31+G(d,p) level obtained with the Onsager model (bond angles are recorded in degrees and bond lengths in angstroms).

TABLE 1: Relative Energies of the Conformers of R1 and R3 (kcal/mol) at the B3LYP/6-311G(2df,p) Level Including Zero-Point Energy Correction at the B3LYP/6-31+G(d,p) Level

system	I	II	III	IV
R1	5.9	0.0	7.1	0.9
R3	9.0	0.0	0.4	12.9

a staggered arrangement of the two H_β's with respect to the OH_x bond. Besides a similar change in bond length as discussed for R1, there is a larger difference in the out-of-plane distortion between R3-I and the other three conformers (R3-II, R3-III, and R3-IV). The dihedral angles involving the amino hydrogens and the two carboxylate oxygen atoms in R3-I differ by at least 10° from the corresponding angles in R3-II, R3-III, and R3-IV. From the relative energies, it can be seen that R3-II and R3-III are more stable than R3-I and R3-IV, due to the intramolecular hydrogen bonding.

Hyperfine Couplings of Radical R1. The calculated full hyperfine tensors of radical R1 are listed in Table 2, together with the experimentally determined tensors for comparison. The isotropic coupling constants of H_α in the four structures of R1 are all close in value and in good agreement with experiment. The computed T_{yy} component has a different sign from the experimental value, and T_{zz} deviates from the experimental value by as much as 6 MHz for all conformers. These deviations could be caused by crystal-packing effects, which are not accounted for in the gas-phase calculations. However, the principal components are in reasonable agreement with the experimental tensors. In addition, the computed average of the methyl proton couplings (the average A_{iso} for H_β's is approximately 65 MHz) in each conformer is in good agreement with the experimental value (69.9 MHz). The deviations of the calculated average anisotropic components seem larger than expected, mainly due to their relatively small values. However, there is no doubt from our calculations that all four conformers are candidates for the molecular structure of radical R1 in the solid state.

TABLE 2: Comparison of Calculated and Experimental[2] Hyperfine Couplings (MHz) of R1

tensor	HFCC	R1-I	R1-II	R1-III	R1-IV	exp
H_α	A_{iso}	−52.0	−54.0	−54.9	−52.9	−56.1
	T_{xx}	−32.5	−32.1	−31.7	−30.9	−31.8
	T_{yy}	−1.4	−1.7	−1.8	−2.1	+3.9
	T_{zz}	33.9	33.8	33.5	33.0	27.9
	A_{xx}	−84.5	−84.0	−86.6	−83.5	−87.9
	A_{yy}	−53.4	−52.8	−56.7	−54.7	−52.7
	A_{zz}	−18.1	−17.8	−21.4	−21.4	−28.3
$H_{\beta1}$	A_{iso}	1.7	1.7	2.0	1.5	
	T_{xx}	−3.9	−4.0	−3.9	−3.6	
	T_{yy}	−2.8	−2.8	−3.4	−3.4	
	T_{zz}	6.7	6.8	7.3	7.1	
$H_{\beta2}$	A_{iso}	96.3	96.9	93.6	97.0	
	T_{xx}	−4.8	−4.8	−4.7	−4.8	
	T_{yy}	−3.0	−3.0	−3.1	−3.0	
	T_{zz}	7.8	7.8	7.8	7.8	
$H_{\beta3}$	A_{iso}	97.5	98.3	95.2	98.6	
	T_{xx}	−4.8	−4.8	−4.6	−4.8	
	T_{yy}	−3.0	−3.1	−3.1	−3.1	
	T_{zz}	7.9	7.9	7.7	7.9	
H_β(av)	A_{iso}	65.2	65.6	63.4	65.7	69.9
	T_{xx}	−4.5	−4.5	−4.5	−4.4	−2.6
	T_{yy}	−2.9	−3.0	−3.2	−3.2	−2.3
	T_{zz}	7.5	7.5	7.5	7.6	4.8

It has been proposed[6] that R1 is generated from a primary carboxylate anion radical (Figure 5) through a deamination reaction. Mayagawa et al.[8] raised an interesting question of specific proton transfer in irradiated crystalline L-α-alanine at low temperatures and concluded through an EPR study at 80 K that the transferred proton specifically binds to the O_2 atom in the COO plane in a position directed toward O_1. Later, Muto et al.[11] reexamined this problem at 77 K using EPR and ENDOR techniques and obtained the opposite conclusion that the

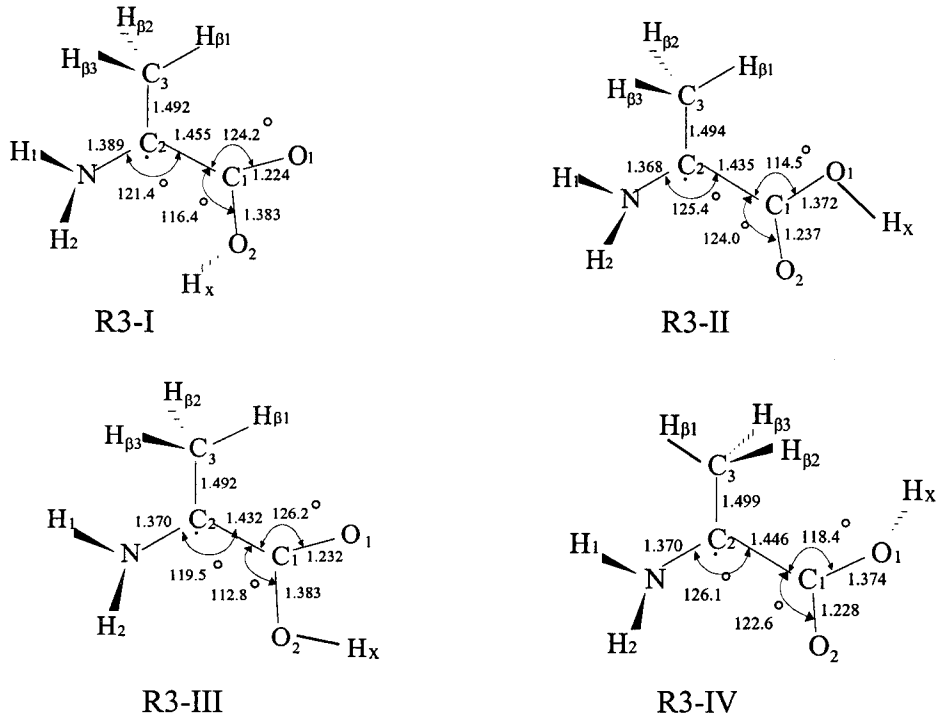

Figure 4. Optimized structures for R3 at the B3LYP/6-31+G(d,p) level (bond angles are recorded in degrees and bond lengths in angstroms).

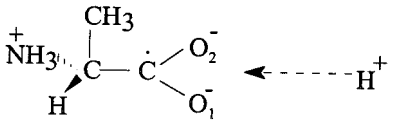

Figure 5. Proton-transfer to the carboxylate anion radical.

TABLE 3: Comparison of Calculated and Experimental[2] Hyperfine Couplings (MHz) of R2

tensor	A_{iso}^{cal}	T_{xx}^{cal}	T_{yy}^{cal}	T_{zz}^{cal}	A_{iso}^{exp}	T_{xx}^{exp}	T_{yy}^{exp}	T_{zz}^{exp}
H_1	2.4	−5.6	−4.9	10.6	86.3	−6.9	−2.7	9.5
H_2	69.9	−4.9	−4.5	9.4	30.2	−6.1	−4.7	10.7
H_3	69.9	−4.8	−4.5	9.3	10.2	−4.9	4.8	9.7
H_{amino}(av)	47.4	−5.1	−4.6	9.8	42.2	−6.0	−4.1	10.0
$H_{\beta 1}$	2.2	−4.1	−3.9	8.0				
$H_{\beta 2}$	95.5	−4.6	−3.4	8.0				
$H_{\beta 1}$	95.7	−4.6	−3.4	8.0				
H_{β}(av)	64.5	−4.3	−3.6	8.0	70.8	−2.9	−2.7	5.6

transferred proton stereospecifically attaches to O_1 along a direction perpendicular to the COO plane and is trapped outside the COO plane. This arrangement was supported by a large positive isotropic coupling assigned to the transferred proton at 77 K. If R1 is formed by a deamination reaction from the stereospecifically proton-transferred carboxylate anion radical, there will be only one conformer corresponding to R1. However, the calculated HFCCs suggest that the four conformers of R1 could exist simultaneously. In addition, since no evidence exists to exclude a possible proton transfer to O_1 and O_2 at 295 K, there could be an equilibrium between the four conformations. The ratio of the four conformers will depend on the individual reaction pathway. Also, it can be seen from the calculations that this problem cannot be solved by a proton ESR study, because the proton couplings of all conformers are very close to each other.

Hyperfine Coupling of Radical R2. In Table 3, the computed full coupling tensor from the optimized structure of R2 is listed, along with the experimental hyperfine coupling values for comparison. For all of the protons of the amino group, great discrepancies between the computed isotropic HFCCs and the experimental values were found. However, the average of the three calculated amino proton isotropic HFCCs (47.4 MHz) is quite close to the average of the three experimental couplings (42.2 MHz), and the averages of the anisotropic couplings are also in good agreement. Despite the above deviations, all the calculated anisotropic components of the amino protons are in good agreement with the corresponding experimental values. The average of the calculated isotropic coupling constants for the three methyl protons (64.5 MHz) is very close to the experimental average (70.8 MHz). In addition, good agreement for the anisotropic components of the methyl protons is found. These observations confidently show that the optimized structure of radical R2 accounts for the hyperfine couplings in the crystalline environment except for the isotropic couplings of the three amino group protons. This prompts a careful study of the effects of the rotation about the NC_2 bond on the amino proton HFCCs.

The difference between experiment and theory is suggested to arise from the relative orientation of the three amino protons in the L-α-alanine crystals. A detailed investigation of the rotational effects of the amino group about the NC_2 bond on the isotropic HFCCs of the amino protons supports this idea. Figure 6 shows the variation in the three amino proton HFCCs as a function of the rotation angle. The rotation of the amino group was carried out by increasing the dihedral angle $H_1NC_2C_1$ by 30° starting from $H_1NC_2C_1 = 0.0°$. From the curve, it can be seen that the isotropic HFCCs of the three amino protons change dramatically, but the anisotropic components fluctuate very little (not shown). This is not surprising since the isotropic component of the HFCC is calculated by summing the contributions only at one particular point in space, while the anisotropic components are computed by integrating over all space. Interestingly, at $H_1NC_2C_1 \approx 40°$, there is an excellent fit of the calculated isotropic couplings [H_1 (30 MHz), H_2 (12 MHz), and H_3 (86 MHz)] to the experimental values (30.2, 10.2, and 86.3 MHz). Thus, it can be concluded that the configuration at $H_1NC_2C_1 \approx 40°$ corresponds to the structure of R2 in the L-α-alanine crystal at 295 K, in which the amino protons are fixed

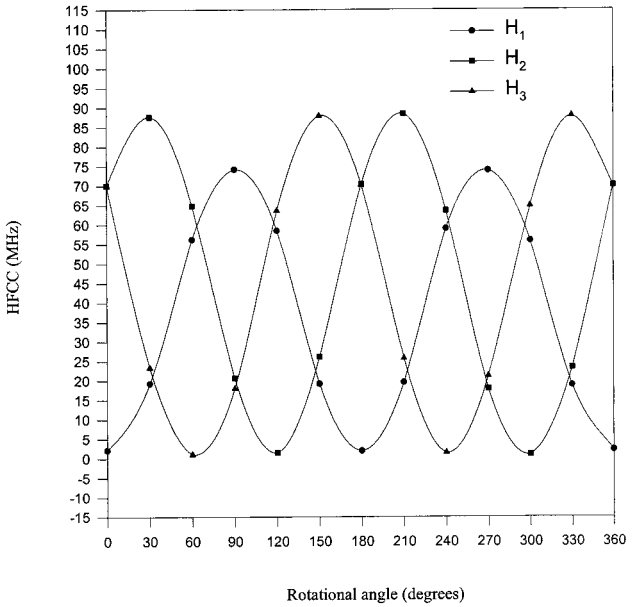

Figure 6. Amino proton HFCCs versus the rotation angle about the NC_2 bond for R2.

TABLE 4: Comparison of Calculated and Experimental[2] Hyperfine Couplings (MHz) of R3

tensor	HFCC	R3-I	R3-II	R3-III	R3-IV	exp
$H_{\beta 1}$	A_{iso}	1.5	2.0	46.9	19.0	
	T_{xx}	−3.9	−3.4	−3.7	−3.5	
	T_{yy}	−2.7	−3.2	−2.7	−3.2	
	T_{zz}	6.6	6.6	6.4	6.6	
$H_{\beta 2}$	A_{iso}	61.1	61.2	56.0	71.7	
	T_{xx}	−3.5	−3.3	−3.5	−3.5	
	T_{yy}	−3.2	−3.0	−2.8	−2.9	
	T_{zz}	6.7	6.4	6.3	6.4	
$H_{\beta 3}$	A_{iso}	60.5	43.7	1.4	15.7	
	T_{xx}	−3.6	−3.5	−3.5	−3.3	
	T_{yy}	−2.9	−2.8	−2.7	−2.8	
	T_{zz}	6.6	6.3	6.2	6.1	
H_{β}(av)	A_{iso}	41.3	35.6	34.8	35.4	39.5, 33.1
	T_{xx}	−3.7	−3.4	−3.6	−3.4	−2.7, −2.3
	T_{yy}	−3.2	−3.0	−2.7	−3.0	−2.2, −2.3
	T_{zz}	6.6	6.3	6.3	6.4	5.0, 4.6

by intermolecular hydrogen bonds. Also, it can be concluded that the Onsager model satisfactorily describes the zwitterionic structure of the amino acid radicals, which is required in order to accurately calculate the HFCCs. Since the experimental results can be explained through a rotation study with this solvation model, more computationally demanding models do not need to be investigated.

Hyperfine Coupling of R3. The computed full coupling tensors of R3 and the experimentally determined tensors are listed in Table 4. Experimentally, two coupling tensors were elucidated and assigned to a rapidly rotating methyl group. Investigation of the average of the calculated methyl proton isotropic HFCCs in the four conformers of R3 isolates the conformers into two groups. One group contains only R3-I with an averaged methyl proton isotropic HFCC equal to 41.3 MHz, which is in excellent agreement with one of the experimental values (39.5 MHz). The second group includes R3-II, R3-III, and R3-IV with an averaged methyl proton isotropic HFCC of approximately 35 MHz, which is in excellent agreement with the second experimental value (33.1 MHz). The largest deviation is less than 1.6 MHz. In addition, all of the anisotropic components for both group one and group two are in nearly perfect agreement with the corresponding experimental values. This leads to the conclusion that at least two conformers of R3 exist in the irradiated L-α-alanine crystals at 295 K. R3-I could be one conformer, and the second conformer could be either R3-II, R3-III, or R3-IV. Another possibility is that the observed spectra arise from a mixture of all four conformations.

TABLE 5: Sum of the Three Bond Angles (deg) of the Amino Group and the NC_2 Bond Length in R3 (Å)

structure	$\angle H_1NC_2$	$\angle H_2NC_2$	$\angle H_1NH_2$	sum	$R(NC_2)$
R3-I	116.1	117.4	112.4	345.9	1.389
R3-II	120.1	116.8	117.8	354.7	1.368
R3-III	119.6	117.1	117.1	355.4	1.370
R3-IV	119.9	117.3	117.3	352.7	1.370

TABLE 6: Spin Density from DFT(PWP86) and Semiempirical[2] Calculations on the C_2, N, and O Atoms in R3

atom	R3-I	R3-II	R3-III	R3-IV	semiempirical
C_2	0.597	0.519	0.521	0.537	0.45
N	0.162	0.232	0.222	0.235	0.20
$O_1 + O_2$	0.203	0.185	0.206	0.181	
$O^{carbonyl}$	0.188	0.146	0.183	0.181	0.25

Comparison of the molecular structure of R2 with that of R3-I leads to a possible mechanism for the formation of R3-I. In particular, R3-I can be formed from radical R2 through an intramolecular proton transfer. Alternatively, R2 could be formed from R3-I through an intramolecular proton transfer. However, the other three conformers appear to be products of intermolecular proton transfer.

A more interesting correlation of the radical structure to the HFCCs is found when the coplanarity of H_1, H_2, N, and C_2 is examined. Table 5 lists the sum of the three bond angles of the amino group and the NC_2 bond length in R3-I, R3-II, R3-III, and R3-IV. From the results, it can be seen that the amino group of the four conformers tends to be planar, but the sums of the three bond angles fall into two groups. Only R3-I is in the first group, while R3-II, R3-III, and R3-IV are in the second group. The sum of the three bond angles in R3-I is at least 6.8° less than that of the second group. This indicates a larger π-conjugation in the second group. This statement is supported by comparison of the NC_2 bond lengths of the four conformers. All the NC_2 bond lengths in the second group are approximately 0.02 Å shorter than that of R3-I. Thus, the difference in the isotropic HFCCs of the two groups can be interpreted by the spin polarization of the unpaired α spin electron at the C_2 atom. More specifically, the more planar the amino group, the more easily the spin polarization from the lone pair electrons of the N atom can occur. Consequently, the more planar the amino group in R3, the lower the α (positive) spin density on the C_2 atom, and the more α spin density on the N atom. Hence, the methyl proton isotropic HFCC will be smaller in the more planar radicals.

Table 6 lists the spin density of the N, C_2, and O atoms in R3, together with the semiempirical molecular orbital values[2] for comparison. It can be seen that R3-I has a larger spin density on the C_2 atom than the members of the second group. Thus, R3-I possesses a larger methyl proton isotropic HFCC than R3-II, R3-III, and R3-IV due to a greater distortion at the amino group, and therefore less spin polarization can occur. Also, it can be seen that density-functional theory calculations give a much better resolution of the spin density distribution compared with the semiempirical methods. The DFT calculations presented herein predict that the spin density residing on C_2 in the four conformers is greater than 51%. The total spin density on O_1 and O_2 is between 18.1% and 20.6%, and the spin density on the single carbonyl oxygen is less than 18.8%. The N spin density is between 16.2% and 23.5%. These predictions are

numerically different from the semiempirical molecular orbital values (about 45%, 25%, and 20% for C_2, carbonyl oxygen, and N atom, respectively).

Conclusions

The geometries and hyperfine coupling constants of the radiation products of L-α-alanine at 295 K have been computed using density-functional theory. The calculated results have been compared with the experimental values obtained from X-irradiated crystals of L-α-alanine at 295 K. The three main radiation products (R1, R2, and R3) have been discussed.

Four conformations of R1 were optimized, and their hyperfine couplings support the experimental assignment to this radical. Unusual discrepancies between the calculated and the experimental values of the T_{yy} and T_{zz} anisotropic components for H_α were observed. These differences could be caused by crystal-packing effects that are not accounted for in the calculations.

The standard Onsager model with a dielectric constant of 78.39 predicts a planar zwitterionic structure for R2. A careful study of the rotational effects of the amino group on the amino proton hyperfine couplings shows that the conformation with $H_1NC_2C_1 \approx 40°$ corresponds to the R2 structure in the L-α-alanine crystals, in which the amino protons are fixed by the intermolecular hydrogen bonds. Thus, the geometry obtained from the Onsager model is adequate to describe the HFCCs in this radical, and more complex solvation models are not required to explain experimental results. The calculated hyperfine couplings of R2 show that the crystal environment has little effect on the alanine radical in its zwitterionic form, consistent with a previous investigation on the glycine radical.[35]

Four conformers were investigated for radical R3 in order to provide much more information about the structure of this radical. The conformers fall into two groups. The averages of the calculated methyl proton hyperfine couplings of each group match the experimental couplings perfectly. These results give solid support to the experimental assignment of the detected tensors. A very good correlation of the structure of the amino group to the spin polarization of the unpaired electron on the C_2 atom was found. This correlation accounts for the fact that the methyl proton hyperfine couplings of the four conformations of R3 fall into two groups and reproduce the two experimentally distinguishable coupling tensors.

Methodologically, it can be seen that density-functional theory is very successful in predicting the magnetic properties of amino acids. Also, it can be seen that the Onsager model can predict structures for amino acid radicals in their zwitterionic form that are accurate enough to reproduce experimental hyperfine coupling constants.

Acknowledgment. We gratefully acknowledge the Natural Sciences and Engineering Research Council of Canada (NSERC) and the Killam Trust for financial support.

Supporting Information Available: Tables of molecular geometries and total energies for radicals R1−R3. This material is available free of charge via the Internet at http://pubs.acs.org.

References and Notes

(1) Brustolon, M.; Chis, V.; Maniero, A. L.; Brunel, L. *J. Phys. Chem. A* **1997**, *101*, 4887.
(2) Sagstuen, E.; Hole, E. O.; Haugedal, S. R.; Nelson, W. H. *J. Phys. Chem. A* **1997**, *101*, 9763.
(3) Miyagawa, I.; Gordy, W. *J. Chem. Phys*. **1960**, *32*, 255.
(4) Morton, J. R.; Horsfield, A. *J. Chem. Phys*. **1961**, *35*, 1143. Horsfield, A.; Morton, J. R.; Whiffen, D. H. *Mol. Phys.* **1962**, *4*, 425. Horsfield, A.; Morton, J. R.; Whiffen, D. H. *Mol. Phys*. **1962**, *5*, 115.
(5) Miyagawa, I.; Itoh, K. *J. Chem. Phys.* **1962**, *36*, 2157.
(6) Sinclair, J. W.; Hanna, M. W. *J. Phys. Chem*. **1967**, *71*, 84. Sinclair, J. W.; Hanna, M. W. *J. Chem. Phys.* **1969**, *50*, 2152.
(7) Minegishi, A.; Shinozaki, Y.; Meshitsuka, G. *J. Chem. Soc. Jpn*. **1967**, *40*, 1549.
(8) Miyagawa, I.; Tamura, N.; Cook, J. W. *J. Chem. Phys*. **1969**, *51*, 3520.
(9) Davidson, R.; Miyagawa, I. *J. Chem. Phys*. **1970**, *52*, 1727.
(10) Friday, E. A.; Miyagawa, I. *J. Chem. Phys*. **1971**, *55*, 3589.
(11) Muto, H.; Iwasaki, I. *J. Chem. Phys*. **1973**, *59*, 4821.
(12) Muto, H.; Iwasaki, I.; Ohkuma, J. *J. Magn. Reson*. **1977**, *25*, 327.
(13) Kuroda, S.; Miyagawa, I. *J. Chem. Phys*. **1982**, *76*, 3933.
(14) Matsuki, K.; Miyagawa, I. *J. Chem. Phys*. **1982**, *76*, 3945.
(15) Brudstolon, W.; Segre, U. *Appl. Magn. Reson*. **1994**, *7*, 405.
(16) Simmons, J. A. *J. Chem. Phys*. **1962**, *36*, 469.
(17) Arber, J. M.; Sharpe, P. H. G.; Joly, H. A.; Morton, J. R.; Preston, K. F. *Appl. Radiat. Isotop*. **1991**, *42*, 665.
(18) Ciesielski, B.; Wielopolski, L. *Radiat. Res*. **1994**, *140*, 105.
(19) Minegishi, A.; Bergene, R.; Riesz, P. *Int. J. Radiat. Biol*. **1980**, *38*, 627.
(20) Lion, Y.; Denis, G.; Mossoba, M. M.; Riesz, P. *Int. J. Radiat. Biol*. **1983**, *43*, 71.
(21) Sevilla, M. D. *J. Phys. Chem*. **1970**, *74*, 2096.
(22) Sevilla, M. D.; Brook, V. L. *J. Phys. Chem*. **1973**, *77*, 2954.
(23) Sinclair, J. *J. Chem. Phys*. **1971**, *55*, 245.
(24) Box, H. C. *Radiation Effects, ESR and ENDOR Analysis*; Academic Press: New York, 1977; p 120.
(25) Chakraborty, D.; Manogaran, S. *Chem. Phys. Lett*. **1998**, *294*, 56.
(26) Tortonda, F. R.; Pascual-Ahuir, J. L.; Silla, E.; Tuñón, I. *Chem. Phys. Lett*. **1996**, *260*, 21.
(27) Sambrano, J. R.; Sousa, A. R.; Queralt, J. J.; Andres, J.; Longo, E. *Chem. Phys. Lett*. **1998**, *294*, 1.
(28) Tortonda, F. R.; Pascual-Ahuir, J.; Silla, E.; Tuñón, I.; Ramírez, F. J. *J. Chem. Phys*. **1998**, *109*, 592.
(29) Tarakeshwar, P.; Manogaran, S. *THEOCHEM* **1997**, *417*, 255.
(30) Ding, Y.; Krogh-Jespersen, K. *Chem. Phys. Lett*. **1992**, *199*, 261.
(31) Barone, V.; Adamo, C.; Grand, A.; Subra, R. *Chem. Phys. Lett*. **1995**, *242*, 351.
(32) Barone, V.; Adamo, C.; Grand, A.; Jolibois, F.; Brunel, Y.; Subra, R. *J. Am. Chem. Soc.* **1995**, *117*, 12618.
(33) Onsager, L. *J. Am. Chem. Soc*. **1936**, *58*, 1486.
(34) Wong, M. W.; Frisch, M. J.; Wiberg, K. B. *J. Am. Chem. Soc*. **1991**, *113*, 4776. Wong, M. W.; Wiberg, K. B.; Frisch, M. J. *J. Am. Chem. Soc*. **1992**, *114*, 523. Wong, M. W.; Wiberg, K. B.; Frisch, M. J. *J. Am. Chem. Soc.* **1992**, *114*, 1645. Wong, M. W.; Wiberg, K. B.; Frisch, M. J. *J. Chem. Phys*. **1991**, *95*, 8991.
(35) Rega, N.; Cossi, M.; Barone, V. *J. Am. Chem. Soc*. **1998**, *120*, 5723.
(36) Stubbe, J. A. *Annu. Rev. Biochem*. **1989**, *58*, 257.
(37) Davies, M. J.; Fu, S.; Dean, R. T. *Biochem. J*. **1995**, *305*, 643.
(38) Van der Zee, J. *Biochem. J*. **1997**, *322*, 633.
(39) Stadtman, E. R. *Annu. Rev. Biochem*. **1993**, *62*, 797.
(40) Heller, C.; McConnell, H. M. *J. Chem. Phys.* **1960**, *32*, 1535.
(41) Malkin, V. G.; Malkina, O. L.; Eriksson, L. A.; Salahub, D. R. In *Mordern Density Functional Theory, A Tool for Chemistry*; Politzer, P., Seminario, J. M., Eds.; Elsevier: New York, 1995; p 273.
(42) Engels, B.; Eriksson, L. A.; Lunell, S. *Adv. Quantum Chem*. **1997**, *27*, 298.
(43) Wetmore, S. D.; Boyd, R. J.; Eriksson, L. A. *J. Phys. Chem. B* **1998**, *102*, 5369. Wetmore, S. D.; Himo, F.; Boyd, R. J.; Eriksson, L. A. *J. Phys. Chem. B* **1998**, *102*, 7484. Wetmore, S. D.; Boyd, R. J.; Eriksson, L. A. *J. Phys. Chem. B* **1998**, *102*, 7674. Wetmore, S. D.; Boyd, R. J.; Eriksson, L. A. *J. Phys. Chem. B* **1998**, *102*, 9332. Wetmore, S. D.; Boyd, R. J.; Eriksson, L. A. *J. Phys. Chem. B* **1998**, *102*, 10602.
(44) Becke, A. D. *J. Chem. Phys*. **1993**, *98*, 1372.
(45) Lee, C.; Yang, W.; Parr, R. G. *Phys. Rev. B* **1988**, *37*, 785.
(46) Frisch, M. J.; Trucks, G. W.; Schlegel, H. B.; Gill, P. M. W.; Johnson, B. G.; Robb, M. A.; Cheeseman, J. R.; Keith, T. A.; Petersson, G. A.; Montgomery, J. A.; Raghavachari, K.; Al-Laham, M. A.; Zakrzewski, V. G.; Ortiz, J. V.; Foresman, J. B.; Cioslowski, J.; Stefanov, B. B.; Nanayakkara, A.; Challacombe, M.; Peng, C. Y.; Ayala, P. Y.; Chen, W.; Wong, M. W.; Andres, J. L.; Replogle, E. S.; Gomperts, R.; Martin, R. L.; Fox, D. J.; Binkley, J. S.; DeFrees, D. J.; Baker, J.; Stewart, J. P.; Head-Gordon, M.; Gonzalez, C.; Pople, J. A. *Gaussian 94*; Gaussian Inc.: Pittsburgh, PA, 1995.
(47) Perdew, J. P.; Wang, Y. *Phys. Rev. B* **1986**, *33*, 8800.
(48) Perdew, J. P. *Phys. Rev. B* **1986**, *33*, 8822; **1986**, *34*, 7406.
(49) St-Amant, A.; Salahub, D. R. *Chem. Phys. Lett.* **1990**, *169*, 387. Salahub, D. R.; Fournier, R.; Mylynarski, P.; Papai, I.; St-Amant, A.; Ushio, J. In *Density Functional Methods in Chemistry*; Labanowski, J., Andzelm, J., Eds.; Springer-Verlag: New York, 1993. St-Amant, A. Ph.D. Thesis, Université de Montréal, 1991.
(50) Lassmann, G.; Eriksson, L. A.; Himo, F.; Lendzian, F.; Lubitz, W. *J. Phys. Chem. A* **1999**, *103*, 1283.
(51) Eriksson, L. A. *Mol. Phys*. **1997**, *91*, 827.